TMJM THE MINDANAWAN JOURNAL OF MATHEMATICS
OFFICIAL JOURNAL OF THE MINDANAO STATE UNIVERSITY - ILIGAN INSTITUTE OF TECHNOLOGY

Vol. 7 (2025), no. 1, pp. 1–15 ISSN: 2094-7380 (Print) | 2783-0136 (Online)
http://dx.doi.org/10.62071/tmjm.v7i1.719.

Analysis and Simulation of Organism Survival: A Toxicokinetic-Toxicodynamic Model for Substance Exposure

Rohaimah H. Abdul Majid[1,*], Randy L. Caga-anan [2], and Youcef Mammeri[3]

[1,2]Department of Mathematics and Statistics
MSU-Iligan Institute of Technology, 9200 Iligan City, Philippines
rohaimah.abdulmajid@g.msuiit.edu.ph, randy.caga-anan@g.msuiit.edu.ph

[3] Université Jean Monnet, Institut Camille Jordan UMR5208, CNRS, Ecole Centrale de Lyon, INSA Lyon, Universite Claude Bernard Lyon 1, 42023 Saint-Etienne, France
youcef.mammeri@math.cnrs.fr

Received: Received: 1st January 2025 Revised: 11th January 2025

Abstract

This study develops a mathematical model to analyze the effects of chemical exposure on organism population dynamics. Using a set of TK-TD differential equations, the model examines the interactions between chemical concentration, damage, and population survival. Numerical simulations validate the theoretical results and explore the system's behavior under different scenarios. The findings provide insights into the long-term impacts of chemical stress on population resilience and demonstrate the utility of mathematical models for environmental risk assessment.

1 Introduction

Chemical pollutants in the environment have significant impacts on organisms, affecting their physiological, behavioral, and ecological functions. These pollutants, which enter ecosystems through pathways such as soil, water, and air, can cause acute effects like organ failure or mortality, as well as chronic impacts, including developmental delays, impaired reproduction, and increased susceptibility to diseases, see [10]. Furthermore, exposure to these chemicals can lead to broader ecological consequences, disrupting populations and ecosystems, resulting in long-term health issues and ecological imbalances that harm biodiversity and ecosystem stability, see [11].

The toxicity of a chemical pollutant depends on several factors, including its concentration, persistence, and the organism's ability to metabolize or eliminate it. Pollutants such as pesticides, heavy metals, and industrial chemicals can accumulate within organisms, disrupting biochemical pathways and triggering damage that can be difficult to reverse, see [1]. For instance, chronic exposure to sub-lethal doses of contaminants can impair vital physiological processes, resulting in reduced growth rates, diminished fertility, and altered behaviors critical

*Corresponding author
2020 Mathematics Subject Classification: 92D25, 34D20
Keywords and Phrases: Mathematical Model, Chemical Exposure, Population Dynamics, Toxicology
This research is supported by the DOST ASTHRDP SRSF Grant

for survival, see [3]. These impacts highlight the necessity of studying the interaction between chemical pollutants and biological systems.

Ecotoxicological studies have long focused on quantifying the relationships between exposure levels, internal pollutant concentrations, and subsequent biological responses. These studies have revealed threshold concentrations for toxicity and identified key physiological and environmental factors that influence the effects of pollutants on living organisms, see [5]. This field also provides critical insights into how organisms respond to varying doses over time, making it possible to predict long-term outcomes and potential risks to populations and ecosystems. However, bridging these findings into practical tools for predicting the cumulative effects of pollutants remains a pressing challenge.

Addressing this challenge requires an integrative approach that combines experimental observations, ecotoxicological principles, and mathematical modeling. By developing frameworks that simulate the dynamics of pollutant absorption, damage accrual, and survival outcomes, researchers can gain a deeper understanding of how contaminants influence biological systems. Such models provide valuable tools for advancing ecotoxicology, enabling predictions of pollutant impacts across different contexts and informing strategies for environmental management.

The rest of this paper is structured as follows: In section 2, we presents the toxicokinetic-toxicodynamic (TK-TD) model, along with a detailed description of the associated parameters. Section 3 provides a rigorous mathematical analysis, demonstrating the uniqueness, nonnegativity, and boundedness of the solution, as well as investigating the equilibrium points and their stability. Section 4 discusses the results of the simulations, highlighting their consistency with the analytical predictions. Finally, in section 5, we offer our discussion.

2 Mathematical model and its study

2.1 Description of the model

The model employed in this study is based on a toxicokinetic-toxicodynamic (TK-TD) framework, specifically inspired by the General Unified Threshold Model of Survival (GUTS), see [8]. The TK component describes how a chemical substance is absorbed, distributed, and eliminated within an organism, while the TD component captures how chemical exposure impacts the organism's survival and reproduction, see [6]. This model simulates the effects of a chemical substance on a population by describing three interrelated dynamic variables: the internal concentration of the chemical within the organisms (C), the damage inflicted by the substance (D), and the cumulative risk posed to the population (H). The flowchart of the model is shown in Figure 1, and the parameters are outlined in Table 1.

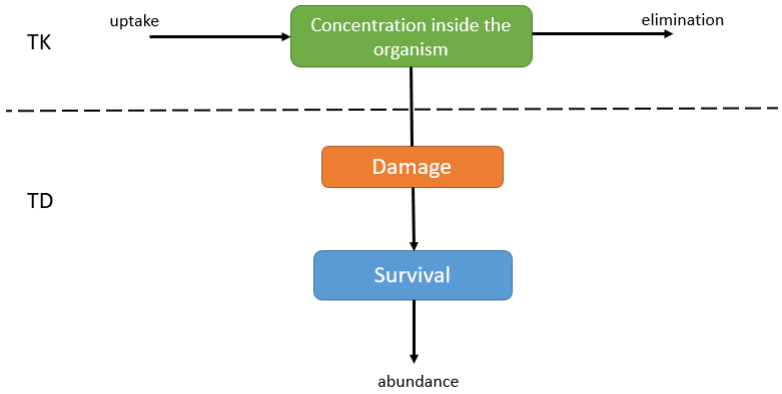

Figure 1: Schematic representation of the GUTS-model.

The model is governed by the following system of ordinary differential equations:

$$\frac{dC}{dt} = (k_0 C_{out} - k_1 C(t))\,\mathbf{1}_{t \le t_c} - k_2 C(t)\mathbf{1}_{t > t_c} \quad (1)$$

$$\frac{dD}{dt} = k_a C(t) - k_r D(t) \quad (2)$$

$$\frac{dH}{dt} = k_h \max(D(t) - D_c, 0) + h(t) \quad (3)$$

Each equation corresponds to a distinct biological process. The first equation models the internal concentration of the chemical, influenced by external exposure (C_{out}), absorption rate (k_0), and decay rates (k_1 and k_2), with the decay switching at a specific threshold time or critical time (t_c). The second equation tracks the accumulation and decay of damage, driven by the absorption rate into the organism (k_a) and the natural repair mechanisms (k_r). Finally, the third equation describes the cumulative risk to the population, which depends on the growth rate of risk (k_h) above a threshold damage level (D_c) and an external hazard function (h).

Table 1: Description of the parameters

Parameters	Description
t_c	Critical time
C_{out}	External concentration
k_0	Absorption rate constant
k_1	Elimination rate constant ($t \le t_c$)
k_2	Elimination rate constant ($t > t_c$)
k_a	Damage accumulation rate constant
k_r	Damage recovery constant
k_h	Mortality rate
D_c	Threshold effects
$h(t)$	Hazard function

The model extends to predict the organism population size $N(t)$ over time. The survival

http://dx.doi.org/10.62071/tmjm.v7i1.719

probability $S(t)$ is determined by the cumulative risk $H(t)$ as follows:

$$S(t) = \exp(-H(t)), \text{ and } N(t) = S(t)N_0.$$

where N_0 is the initial population size. This formulation reflects the combined influence of risk accumulation and initial population size on long-term survival.

3 Qualitative Analysis

In this section, the model is qualitatively analyzed to investigate the well-posedness and stability of the equilibrium points.

3.1 Well-posedness

In analyzing the interactions between chemical accumulation, damage, and population dynamics of organisms, it is vital to ensure the model produces a single, well-defined solution for any given initial conditions and that all variables remain nonnegative and bounded. This guarantees the reliability of the model's predictions and the consistency of numerical simulations. The following theorems establish these foundational aspects:

Theorem 3.1. *Given a nonnegative and bounded initial datum, the system of equations (1) - (3) has a unique global in time solution. Moreover the solution remains nonnegative and bounded for all time $t \geq 0$.*

Proof. Since the right-hand side of the system of equations (1) - (3) is continuous with continuous partial derivatives, by Cauchy-Lipschitz's theorem, the system of equations (1) - (3) has a local in time unique solution.

The variables $C(t)$, $D(t)$, and $H(t)$ represent physical or biological quantities. These quantities are inherently non-negative since negative values would not have any physical or biological meaning. Hence, we assume that $C(0) \geq 0$, $D(0) \geq 0$, and $H(0) \geq 0$. Consider the equation (1), for $t \leq t_c$,

$$\frac{dC}{dt} = k_0 C_{out} - k_1 C(t).$$

This implies that

$$\frac{dC}{dt} + k_1 C(t) = k_0 C_{out}.$$

The solution to this linear first order equation in C is given by

$$\begin{aligned} C(t) &= C(0)e^{-k_1 t} + \frac{k_0 C_{out}}{k_1}(e^{k_1 t} - 1)e^{-k_1 t} \\ &= C(0)e^{-k_1 t} + \frac{k_0 C_{out}}{k_1}(1 - e^{-k_1 t}). \end{aligned}$$

Since $C(0) \geq 0$, it follows that $C(t) \geq 0$. Notice that

$$|C(t)| \leq \max\left\{C(0), \frac{k_0 C_{out}}{k_1}\right\}.$$

Hence, $C(t)$ is bounded. For $t > t_c$, the system (1) becomes

$$\frac{dC}{dt} + k_2 C(t) = 0,$$

and

$$C(t) = C(t_c)e^{-k_2(t-t_c)},$$

where

$$C(t_c) = C(0)e^{-k_1 t_c} + \frac{k_0 C_{out}}{k_1}(1 - e^{-k_1 t_c}) \geq 0.$$

Hence, $C(t) \geq 0$. Since the solution $C(t)$ decays exponentially to zero, $C(t)$ is bounded. Now, from equation (2) of the model, we get

$$\frac{dD}{dt} + k_r D(t) = k_a C(t).$$

Solving the above equation using the same method, we have

$$D(t) = D(0)e^{-k_r t} + k_a e^{-k_r t} \int_0^t e^{k_r \tau} C(\tau)\, d\tau.$$

Since $D(0) \geq 0$, $C(\tau) \geq 0$, it follows that $D(t) \geq 0$ for all time t. Moreover, $D(t)$ is bounded since $C(t)$ is bounded. Finally, from the last equation (3) of the system,

$$\frac{dH}{dt} = k_h \max(D(t) - D_c, 0) + h(t).$$

Integrating both sides from 0 to t, we have

$$H(t) - H(0) = \int_0^t (k_h \max(D(\tau) - D_c, 0) + h(\tau))\, d\tau$$

$$H(t) = H(0) + \int_0^t (k_h \max(D(\tau) - D_c, 0) + h(\tau))\, d\tau$$

Note that $H(0) \geq 0$, $\max(D(\tau) - D_c, 0) \geq 0$, and $h(t) \geq 0$, hence $H(t) \geq 0$ for all time t. Furthermore $H(t)$ is bounded since $D(t)$ and $\max(D(\tau) - D_c, 0)$ are bounded. □

3.2 Qualitative Behavior

The equilibrium is solution to the system that is constant for any time t. That is, a solution

$$(C^*, D^*, H^*)$$

such that

$$\frac{dC}{dt} = \frac{dD}{dt} = \frac{dH}{dt} = 0.$$

Analyzing equilibrium points is essential to understanding the long-term behavior of the system, as they represent steady-state conditions where the dynamic variables no longer change over time. These points provide insights into the stability of the system and the potential impact of chemical exposure on organism populations. In this section that hazard does not occurs by assuming $h \equiv 0$. The following theorem identifies the equilibrium points of the system.

Theorem 3.2. *System (1) - (3) has two equilibrium points (C^*, D^*, H^*), given by, for $t \leq t_c$,*

$$x_0 = \left(\frac{k_0}{k_1} C_{out}, \frac{k_a k_0}{k_r k_1} C_{out}, H_0\right),$$

and for $t > t_c$

$$x_0 = (0, 0, H_0).$$

http://dx.doi.org/10.62071/tmjm.v7i1.719

Proof. Let (C^*, D^*, H^*) be an equilibrium point. Then, $\frac{dC}{dt} = \frac{dD}{dt} = \frac{dH}{dt} = 0$. That is,

$$\begin{aligned} 0 &= (k_0 C_{out} - k_1 C^*)\, \mathbf{1}_{t \le t_c} - k_2 C^* \mathbf{1}_{t > t_c} && (4)\\ 0 &= k_a C^* - k_r D^* && (5)\\ 0 &= k_h \max(D^* - D_c, 0). && (6) \end{aligned}$$

Case 1: $t \le t_c$.
From equation (4), and (5), we obtain

$$C^* = \frac{k_0}{k_1} C_{out}\ , \quad D^* = \frac{k_a k_0}{k_r k_1} C_{out}$$

From equation (6), if $\frac{k_a k_0}{k_r k_1} C_{out} \le D_c$, then $\max(D^* - D_c, 0) = 0$. On the other hand, if $\frac{k_a k_0}{k_r k_1} C_{out} > D_c$, then $\max(D^* - D_c, 0) = D^* - D_c > 0$, and there is no equilibrium in this case.

Case 2: $t > t_c$.
From equation (4), (5) and (6), we get

$$C^* = 0\ , \quad D^* = 0.$$

Then $\max(D^* - D_c, 0) = 0$ and the third equation is satisfied. □

3.3 Stability Analysis

Understanding the stability of equilibrium points is essential for assessing how the system responds to small disturbances and provides insights into the resilience of the population under chemical stress. The following theorems confirm the stability of the equilibrium points.

Theorem 3.3. *If $t_c = +\infty$, the equilibrium point*

$$x_0 = \left(\frac{k_0}{k_1} C_{out}, \frac{k_1 k_0}{k_r k_1} C_{out}, H_0 \right),$$

is locally asymptotically stable.

Proof. The Jacobian matrix if $t_c = +\infty$ is given by

$$\mathcal{J}(x_1, x_2, x_3) = \begin{bmatrix} -k_1 & 0 & 0 \\ k_a & -k_r & 0 \\ 0 & k_h & 0 \end{bmatrix}.$$

Evaluating the Jacobian matrix at the equilibrium point x_0 gives us

$$\mathcal{J}^*(x_1, x_2, x_3) = \begin{bmatrix} -k_1 & 0 & 0 \\ k_a & -k_r & 0 \\ 0 & k_h & 0 \end{bmatrix}.$$

Let the eigenvalues be $\lambda_1, \lambda_2, \lambda_3$ of the Jacobian matrix. Solving the eigenvalues of $\mathcal{J}(x_1, x_2, x_3)$, we have

$$\begin{aligned} \det|\mathcal{J}^* - \mathrm{I}\lambda| &= \det \begin{bmatrix} -k_1 - \lambda & 0 & 0 \\ k_a & -k_r - \lambda & 0 \\ 0 & k_h & -\lambda \end{bmatrix} \\ &= (-k_1 - \lambda) \cdot \det \begin{bmatrix} -k_r - \lambda & 0 \\ k_h & -\lambda \end{bmatrix} - 0 \cdot \det \begin{bmatrix} k_a & 0 \\ 0 & -\lambda \end{bmatrix} + 0 \cdot \det \begin{bmatrix} k_a & -k_r - \lambda \\ 0 & k_h \end{bmatrix} \\ &= (-k_1 - \lambda)(-k_r - \lambda)(-\lambda). \end{aligned}$$

Hence, the eigenvalues of $\mathcal{J}(x_1, x_2, x_3)$ are

$$\lambda_1 = -k_1 \ , \quad \lambda_2 = -k_r \ , \quad \lambda_3 = 0.$$

Since the eigenvalues are either negative or zero, the equilibrium

$$x_0 = \left(\frac{k_0}{k_1} C_{out}, \frac{k_1 k_0}{k_r k_1} C_{out}, H_0\right),$$

is locally asymptotically stable. □

Theorem 3.4. *If t_c is finite, the equilibrium point $x_0 = (0, 0, H_0)$ is locally asymptotically stable.*

Proof. The Jacobian matrix is given by

$$\mathcal{J}(x_1, x_2, x_3) = \begin{bmatrix} -k_2 & 0 & 0 \\ k_a & -k_r & 0 \\ 0 & k_h & 0 \end{bmatrix}.$$

Using the same method with the previous theorem, the eigenvalues of $\mathcal{J}(x_1, x_2, x_3)$ are

$$\lambda_1 = -k_2 \ , \quad \lambda_2 = -k_r \ , \quad \lambda_3 = 0.$$

Since the eigenvalues are either negative or zero, the equilibrium

$$x_0 = (0, 0, H_0),$$

is locally asymptotically stable. □

4 Numerical simulations

The numerical simulations in this study are conducted to verify the results of the mathematical analysis. By solving the system of equations numerically, we can observe the dynamics of chemical concentration, damage, and population survival over time. These simulations help confirm the accuracy and consistency of the theoretical predictions, providing a clear picture of how the system behaves under various conditions. The parameter values were thoughtfully chosen to capture moderate environmental effects, see [4, 9]. The summary of the assumed values is shown in Table 2.

Table 2: Assumed values of parameters.

Parameters	Description	Assumed Value
C_{out}	External concentration	1.25
k_0	Absorption rate constant	0.5
k_1	Elimination rate constant ($t \leq t_c$)	0.2
k_2	Elimination rate constant ($t > t_c$)	0.1
k_a	Damage accumulation rate constant	0.3
k_r	Damage recovery constant	0.2
k_h	Mortality rate	0.4
D_c	Threshold effects	5

http://dx.doi.org/10.62071/tmjm.v7i1.719

The assumed parameter values in Table 2 provide the foundation for analyzing how the model responds under various scenarios. To validate the agreement between the simulations and the theoretical analysis, we explore specific cases that represent different environmental and chemical exposure conditions. These cases allow for a detailed examination of the system's dynamics.

Case 1: $t_c = +\infty$, and $h = 0$.

In the first case, we examine the situation where the critical time t_c is infinitely large, and no additional baseline hazard is introduced.

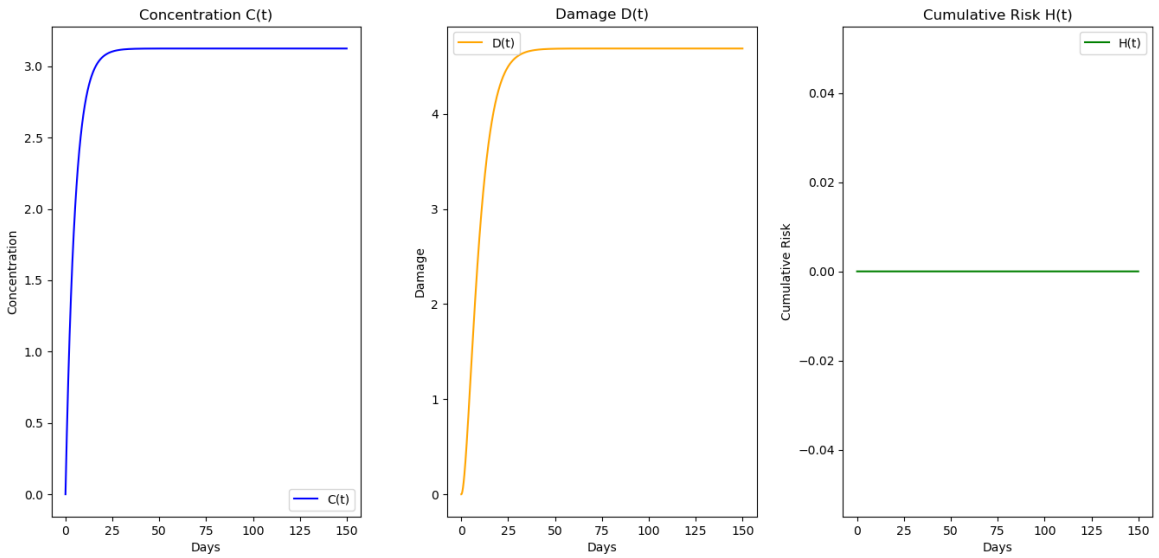

Figure 2: Temporal evolution of internal concentration $C(t)$, damage $D(t)$, and cumulative risk $H(t)$, all converging to their respective equilibrium values.

Figure 2 shows that $C(t)$ rises initially due to C_{out}, then decays with k_1 at a steady state. Moreover, it stabilizes near its equilibrium value:

$$C^* = \frac{k_0}{k_1} C_{out} = \frac{0.5}{0.2} \cdot 1.25 = 3.125.$$

For $D(t)$, it grows as the chemical concentration is absorbed $(k_a \cdot C(t))$, then decays with kr. The growth slows over time as $C(t)$ approaches equilibrium. $D(t)$ approaches to an equilibrium value as well:

$$D^* = \frac{k_a k_0}{k_1 k_r} C_{out} = \frac{0.3 \cdot 0.5}{0.2 \cdot 0.2} \cdot 1.25 = 4.6875.$$

Since $D^* < D_c = 5.0$, no additional cumulative risk is triggered. Hence, H remains 0 all the time. This result agrees with Theorem 3.3.

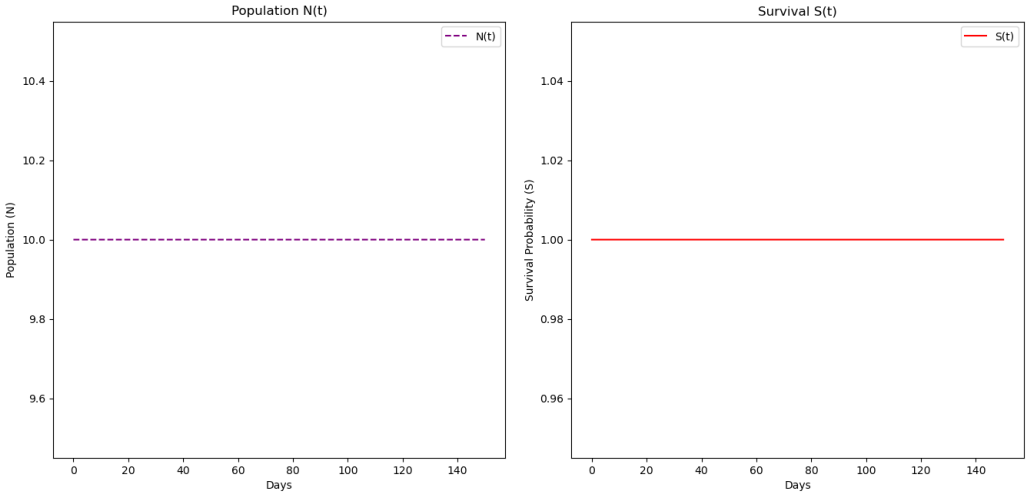

Figure 3: Time-based evolution of survival rate $S(t)$ and organism population, showing no survival loss or population decline due to the absence of cumulative hazard.

Figure 3 shows that $S(t)$ remains constant at 1, as $H(t) = 0$. The organism population experiences no survival loss due to chemical exposure in this case. For the number of population of organism, it remained unchanged over time. With no hazard accumulation, the population is unaffected.

Case 2: $t_c = +\infty$, and $h = \frac{2.0}{1+\exp(-0.1(t-60))}$.

In the second case, we introduce a logistic hazard function for $h(t)$, which models an increasing hazard rate peaking around $t = 60$.

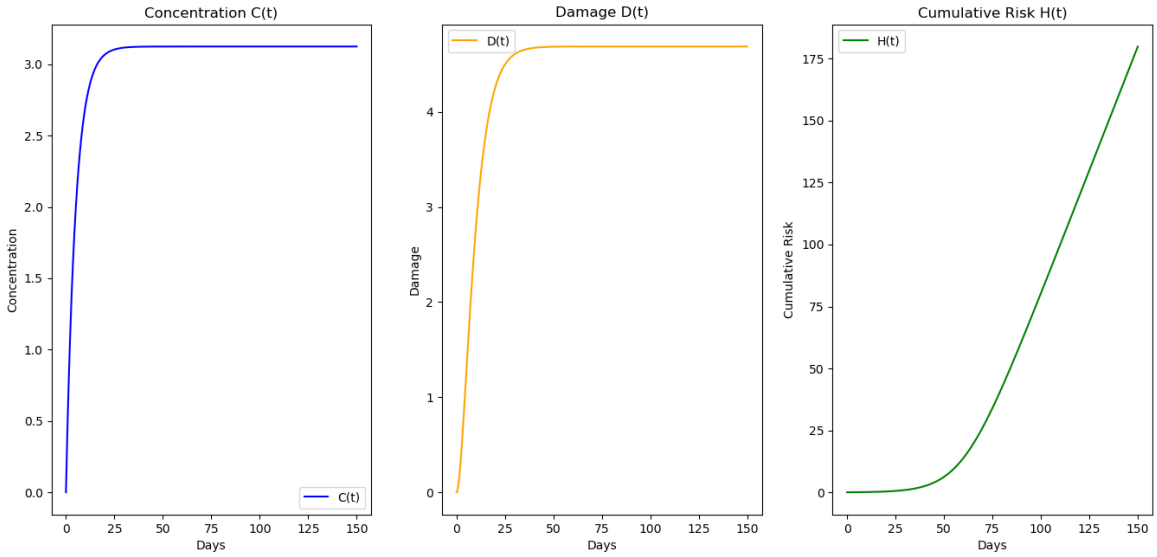

Figure 4: Temporal evolution of internal concentration $C(t)$, damage $D(t)$, and cumulative risk $H(t)$ in the presence of a logistic hazard function.

Figure 4 shows that the hazard function $h(t)$ causes a sharp rise in cumulative risk $H(t)$ despite $D(t)$ staying below D_c, the logistic hazard contributes significantly to cumulative risk

http://dx.doi.org/10.62071/tmjm.v7i1.719

with a value of $H(t) = 179.953$. While the behavior of $C(t)$, and $D(t)$ are similar with the previous case, with equilibrium approaching

$$C^* = 3.125, \quad \text{and} \quad D^* = 4.6875,$$

respectively.

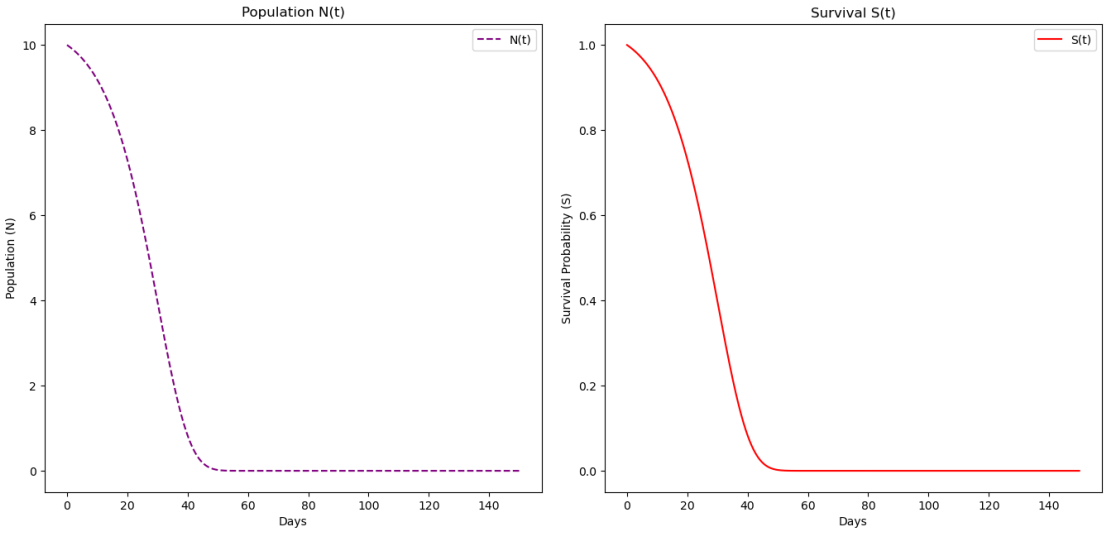

Figure 5: Dynamics of organism population $N(t)$ and survival probability $S(t)$ over time. The exponential decay of survival probability drives changes in population.

Figure 5 shows the decline in both the survival rate $S(t)$ and the population of organism N. $S(t)$ drops near $t = 60$, asymptotically approaching 0 as $H(t)$ grows unbounded. The logistic hazard clearly has strong effects on organism survival. As the survival rate decreases and $H(t)$ increases, the population decreases, unable to sustain itself under high cumulative risk.

Case 3: $t_c = +\infty$, $h = 0$ and $D^* > D_c$.

The third case considers the scenario where the damage exceeds the threshold D_c.

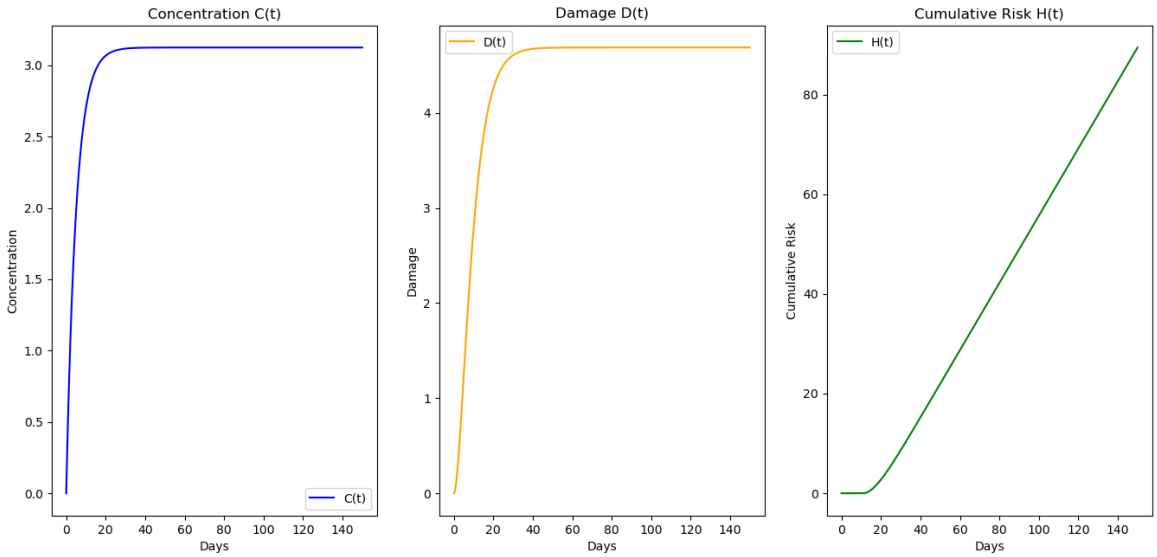

Figure 6: Time series plots of $C(t), D(t)$, and $H(t)$: $C(t)$ stabilizes due to decay dynamics, $D(t)$ reflects cumulative damage, and $H(t)$ rises only when $D(t) > D_c$.

As shown in Figure 6, $C(t)$ rises initially due to the external concentration C_{out}, then stabilizes at $C^* = 3.125$. Similarly, $D(t)$ reaches its equilibrium value $D^* = 4.6875$. However, since D^* exceeds $D_c = 5$, the cumulative risk $H(t)$ begins to increase after the threshold is crossed.

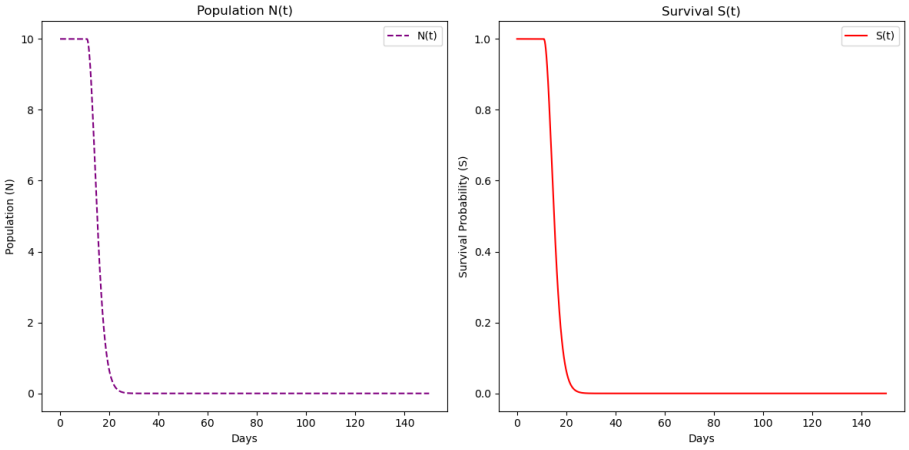

Figure 7: Population $N(t)$ and survival probability $S(t)$ over time: $S(t)$ declines with cumulative risk, driving a reduction in $N(t)$.

Figure 7 shows that as the cumulative risk $H(t)$ increases, $S(t)$ declines exponentially,causing a reduction in the organism population. This result demonstrates the crucial role of damage thresholds in determining whether the cumulative risk reaches levels sufficient to impact the survival and growth of the population.

Case 4: $t_c = 4$, and $h(t) = 0$.

In this case, we introduce a finite critical time $t_c = 4$, and again assume no baseline hazard $(h(t) = 0)$

http://dx.doi.org/10.62071/tmjm.v7i1.719

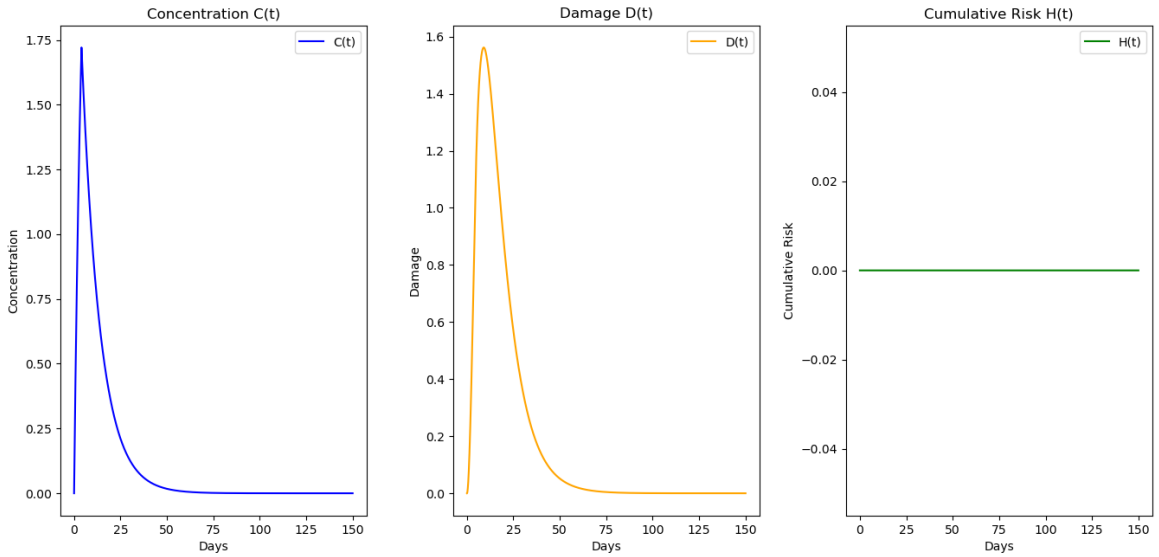

Figure 8: Temporal evolution of internal concentration, damage, and cumulative risk for a finite critical time and no baseline hazard.

The dynamics of $C(t)$ and $D(t)$ are shown in Figures 8. Initially, $C(t)$ increases due to the external concentration C_{out}, and after $t_c = 4$, the elimination rate switches to a slower value k_2, causing $C(t)$ to decrease gradually. Similarly, $D(t)$ increases initially but eventually slows down as the chemical is eliminated from the organism.

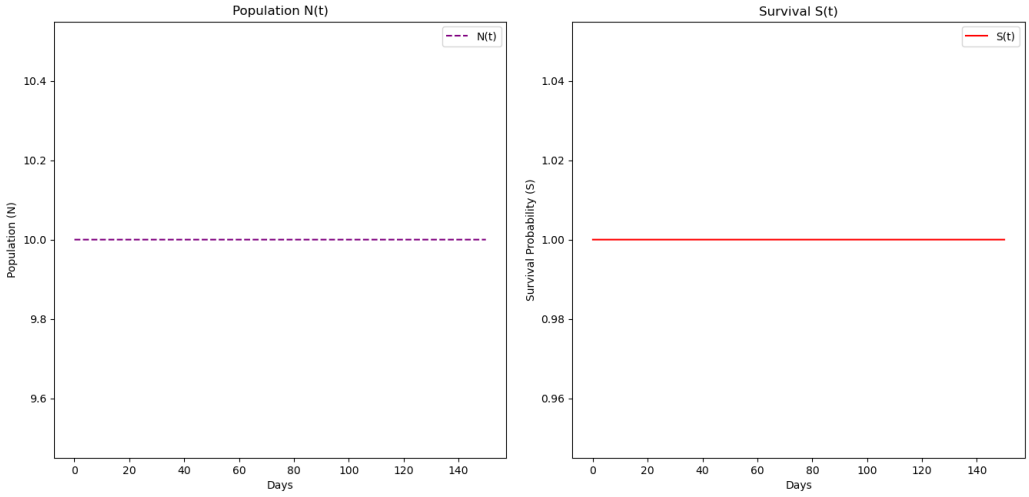

Figure 9: Time evolution of the survival rate $S(t)$ and organism population shows no decline in survival or population due to the lack of cumulative hazard.

Since $H(t) = 0$, $S(t)$ remains at 1, and so N is constant too. The survival of organism is less sensitive to damage under this case, as the fixed $h(t) = 0$ eliminates any baseline hazard contribution.

Case 5: $t_c = 4$, and $h = \frac{2.0}{1+\exp(-0.1(t-60))}$.

The final case introduces both a finite $t_c = 4$ and a logistic hazard function for $h(t)$.

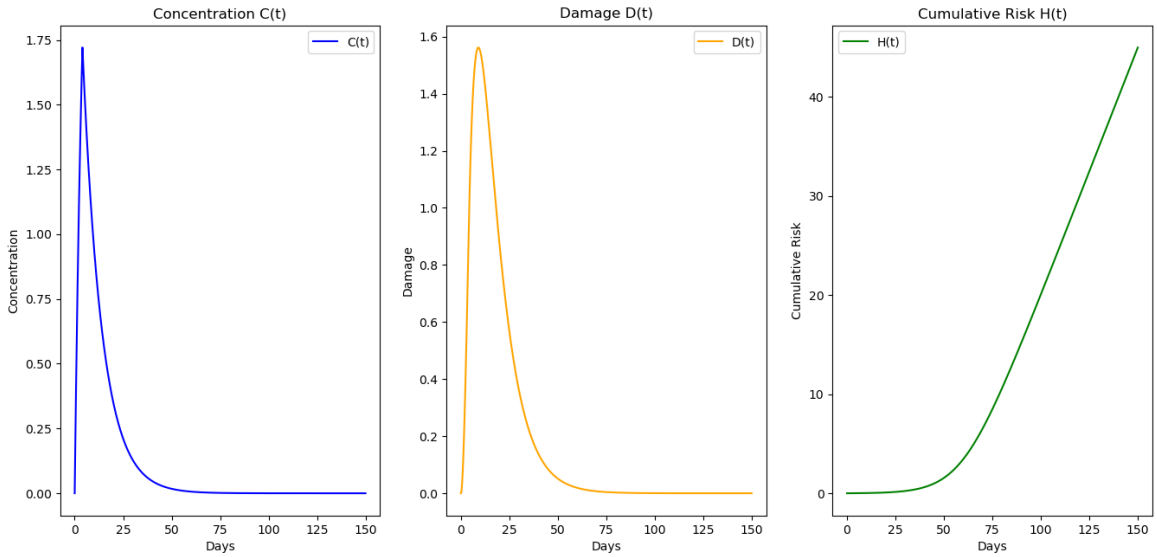

Figure 10: Evolution of internal concentration, damage, and cumulative risk over time for a finite critical time with the introduction of a logistic hazard function.

Figure 10 shows the plot for $C(t)$ and $D(t)$ that remains unchanged compared to the previous case. However, for $H(t)$, it increases due to the influence of the hazard function ($h(t)$), accumulating over time.The sharp rise reflects the significant impact of the hazard function on cumulative risk, potentially affecting survival.

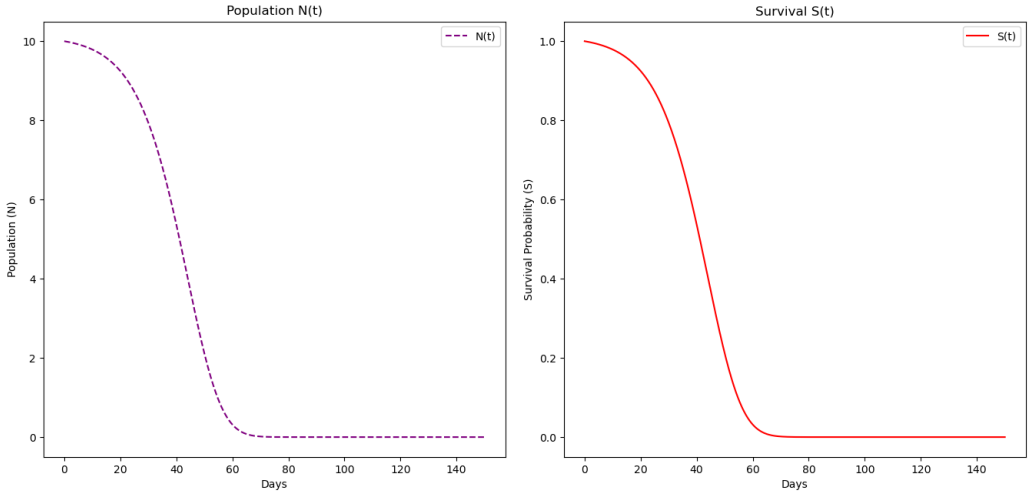

Figure 11: Exponential decline in survival rate $S(t)$ as $H(t)$ increases, leading to a corresponding decrease in organism population $N(t)$.

As $H(t)$ increases, Figure 11 illustrates an exponential decrease in the survival rate $S(t)$. High hazard rates sharply reduce survival, highlighting the severity of the chemical's toxic effects. As $S(t)$ declines, the organism population $N(t)$ also decreases, emphasizing the direct link between survival and population dynamics.

The analysis in Section 3 is consistent with the results from simulations across cases 1 to 5, demonstrating that the model reliably captures the dynamics of organism populations

http://dx.doi.org/10.62071/tmjm.v7i1.719

exposed to varying concentrations of chemical substances. This alignment between theoretical analysis and simulation outcomes reinforces the model's validity, illustrating its effectiveness in quantifying the toxic effects of chemical exposure on organism dynamics. Furthermore, the agreement between analysis and simulation underscores the model's robustness in simulating complex environmental stressors, making it a valuable tool for predicting the impact of chemical pollutants on ecosystems.

5 Discussion

The presented plots collectively describe the dynamics of internal concentration (C), damage (D), cumulative risk (H), survival probability (S), and population size (N) within a modeled toxicokinetic-toxicodynamic framework. The C plot illustrates the evolution of internal concentration over time, showing an initial rise due to external input (C_{out}) followed by a decline governed by the decay rate constants k_1 and k_2. The damage D plot reflects a lagged response to C, as the absorption rate (k_a) and decay rate (k_r) modulate the accumulation and clearance of damage.

Cumulative risk (H) only increases when D surpasses the threshold (D_c), as observed in the H plot. This threshold-dependent growth highlights the nonlinear nature of risk accumulation. The survival probability ($S(t) = \exp(-H(t))$ decreases exponentially as cumulative risk increases, directly impacting the organism population size ($N(t) = N_0 S(t)$). The N plot indicates the decline of the organism population over time, emphasizing the cascading effect of internal processes on population-level outcomes.

When the hazard function (h) is set to zero, the simulations reveal the intrinsic dynamics of the system, providing a baseline for understanding the behavior driven solely by internal processes. This allows for isolating the effects of key parameters, such as k_0, k_1, k_2, and D_c, on the system's dynamics.

Notably, the simulations agree with the analytical expectations derived from the model. For instance, the equilibrium values for C and D align with theoretical predictions based on the model parameters, further validating the consistency between simulation outputs and the underlying mathematical framework. The results also illustrate the cascading effects of toxic exposure, supporting the hypothesized relationships between internal concentration, damage, risk, and population outcomes.

Acknowledgements

The authors are grateful to the anonymous referees for their helpful comments and suggestions.

References

[1] A. Alengebawy, S. T. Abdelkhalek, S. R. Qureshi, and M. Wang, *Heavy metals and pesticides toxicity in agricultural soil and plants: Ecological risks and human health implications*, Toxics **9** (2021), no. 3, 42, doi:10.3390/toxics9030042.

[2] V. I. Arnold, *Ordinary differential equations*, 2nd ed., Springer-Verlag, Berlin, 1992.

[3] M. Bartling, A. Brandt, H. Hollert, and A. Vilcinskas, *Current insights into sublethal effects of pesticides on insects*, Int. J. Mol. Sci. **25** (2024), no. 11, 6007, doi:10.3390/ijms25116007.

[4] B. Bauer, A. Singer, Z. Gao, O. Jakoby, J. Witt, T. Preuss, and A. Gergs, *A toxicokinetic–toxicodynamic modeling workflow assessing the quality of input mortality data*, Environ. Toxicol. Chem. **43** (2023), no. 1, 197–210, doi:10.1002/etc.5761.

[5] R. E. Connon, J. Geist, and I. Werner, *Effect-based tools for monitoring and predicting the ecotoxicological effects of chemicals in the aquatic environment*, Sensors **12** (2012), no. 9, 12741–12771, doi:10.3390/s120912741.

[6] R. Gehring and D. Van Der Merwe, *Toxicokinetic-toxicodynamic modeling*, in: Elsevier eBooks, 2014, doi:10.1016/b978-0-12-404630-6.00008-7.

[7] M. W. Hirsch, S. Smale, and R. L. Devaney, *Differential equations, dynamical systems, and an introduction to chaos*, 3rd ed., Academic Press, Boston, 2013.

[8] T. Jager, C. Albert, T. G. Preuß, and R. Ashauer, *General Unified Threshold model of Survival—a toxicokinetic-toxicodynamic framework for ecotoxicology*, Environ. Sci. Technol. **45** (2011), no. 7, 2529–2540, doi:10.1021/es103092a.

[9] A. Nyman, K. Schirmer, and R. Ashauer, *Toxicokinetic-toxicodynamic modelling of survival of Gammarus pulex in multiple pulse exposures to propiconazole: Model assumptions, calibration data requirements and predictive power*, Ecotoxicology **21** (2012), no. 7, 1828–1840, doi:10.1007/s10646-012-0917-0.

[10] K. Sharma, *Chemical pollution: Definition, causes, effects, prevention*, Science Info, July 16, 2023, scienceinfo.com/chemical-pollution-causes-effects-prevention.

[11] A. Verma, *Environmental impact of chemical pollution*, Pharma Innovation **8** (2019), no. 3, 631–637, doi:10.22271/tpi.2019.v8.i3k.25444.